Structural Chemistry of human RNA Methyltransferases

Matthieu Schapira[1,2,*]

1. Structural Genomics Consortium, University of Toronto, Toronto, ON M5G 1L7, Canada
2. Department of Pharmacology and Toxicology, University of Toronto, Toronto, ON M5S 1A8, Canada

* Correspondence: matthieu.schapira@utoronto.ca

ABSTRACT

RNA methyltransferases (RNMTs) play important roles in RNA stability, splicing, and epigenetic mechanisms. They constitute a promising target class that is underexplored by the medicinal chemistry community. Information of relevance to drug design can be extracted from the rich structural coverage of human RNMTs. In this work, the structural chemistry of this protein family is analyzed in depth. Unlike most methyltransferases, RNMTs generally feature a substrate-binding site that is largely open on the cofactor-binding pocket, favoring the design of bi-substrate inhibitors. Substrate purine or pyrimidines are often sandwiched between hydrophobic walls that can accommodate planar ring systems. When the substrate base is laying on a shallow surface, a 5' flanking base is sometimes anchored in a druggable cavity. The cofactor-binding site is structurally more diverse than in protein methyltransferases, and more druggable in SPOUT than in Rossman-fold enzymes. Finally, conformational plasticity observed both at the substrate and cofactor binding sites may be a challenge for structure-based drug design. The landscape drawn here may inform ongoing efforts towards the discovery of the first RNMT inhibitors.

INTRODUCTION

Methylation of RNA can be categorized based on the nature of the RNA molecule modified (ex: mRNA, tRNA, lncRNA), on the position of the methylation site (at the terminal RNA cap, or internally, along the RNA strand), or on the functional outcome of the methylation event (molecular stabilization, expansion of RNA vocabulary, dynamic regulatory signaling).[1-3] RNA polymerases produce transcripts that carry a terminal 5'-triphosphate (5'-ppp) subsequently converted into guanosine triphosphate (5'-Gppp); ribonucleases generate RNA molecules such as tRNA or rRNA that carry a 5'-monophosphate extremity (5'-p). Diverse combinations of methylation events at 5'-Gppp, 5'-ppp or 5'-p termini by dedicated methyltransferases result in a number of capping configurations that can impact stability, splicing or translation (Figure 1):[1, 4] a common capping cascade in human is the N7 methylation of the terminal guanosine by RNMT[5], followed by 2'O methylation of the ribose at the first and second transcribed nucleotides by CMTR1 and CMTR2 respectively resulting in cap1 (5'-m^7Gppp2'OmX…) and cap2 (5'-m^7Gppp2'OmX2'OmY…) configurations.[6, 7] The m^7G cap (also known as cap0) can also be further dimethylated at N2 by TGS1 to produce a 5'-$m^{2,2,7}$Gppp cap.[8] A more simple cap is the direct methylation of the 5'-γ–phosphate of snRNA by MEPCE.[9] BCDIN3D methylates the 5'-monophosphate terminus of pre-miRNAs produced by the RNase DROSHA, which antagonizes miRNA maturation and regulates miRNA-mediated control of gene expression.[10] Last, piRNAs can be capped by the 2'O-methyltransferase HENMT1 at their 3' terminal nucleotide.[11]

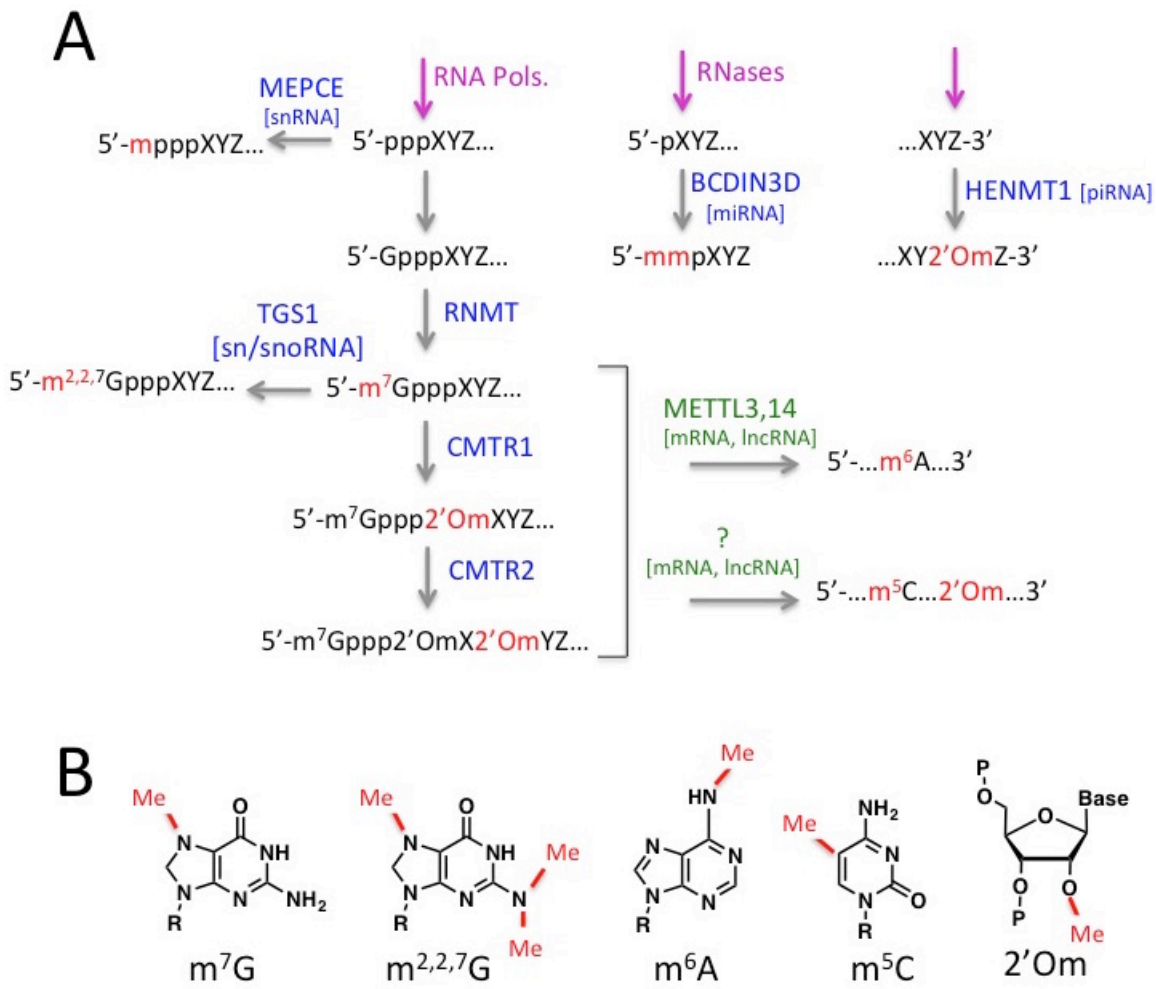

Figure 1: Methylation of mRNA and small RNA. (A) Human RNMTs and reaction products (red) involved in the methylation of mRNA, lnCRNA, snRNA, snoRNA, miRNA, piRNA and in the internal methylation of mRNA and lncRNA are shown. Blue: enzymes involved in RNA capping. Green: Enzymes involved in internal methylation of mRNA and lncRNA. Enzymes currently reported as methylating tRNA or rRNA only are not shown. (B) Chemical structures of methylated bases and ribose.

Internal methylation along mRNA and lncRNA strands are thought to be more dynamic processes than capping events with important roles in epigenetic mechanisms (Figure 1).[12] Methylation at the N6 position of adenines by the METTL3-METTL14 dimer is the most abundant internal post-transcriptional modification in eukaryotic mRNA.[13] The m^{6}A mark can be erased by the

demethylases FTO and ALKBH5 and read by YTH domain containing proteins, thereby controlling mRNA stability and translation efficiency.[14-17] N6-methylation of adenosine also alters local RNA structure, thereby regulating access of RNA binding proteins that control RNA maturation.[18] C5 methylation of cytosine, the landmark posttranslational modification of DNA, is also found in mRNA and lncRNA molecules. NSUN2 could be one of the methyltransferases that write this under-characterized RNA mark.[19] Internal methylation at 2'O was also reported but remains to be characterized.[12]

rRNA and tRNA molecules are also methylated internally. Though not fully understood, the methylation sites on rRNA (>100) may act as a quality control mechanism during ribosome assembly and modulate rRNA structure and function.[20-22] Around 20% of tRNA bases are chemically modified by methyltransferases and other enzymes, which controls molecular stability and translation fidelity.[23-25]

Inhibitors of DNA methyltransferase 1 (DNMT1) as well as small-molecule methyltransferases are approved drugs, and protein methyltransferase (PMT) inhibitors are in clinical trials, but RNA methyltransferases (RNMTs) remain a relatively unexplored target class even though they are implicated in epigenetic mechanisms, splicing events and other biological processes of relevance to drug discovery. No drug-like inhibitor of human RNMTs has been described to date (a few viral RNMT inhibitors have been reported[26, 27]). The epigenetic control of gene expression is a fertile ground for drug discovery. Similarly, RNMT-mediated regulation of mRNA, lncRNA or miRNA maturation and stability could provide novel opportunity for translational research. For instance, BCDIN3D negatively regulates miRNA maturation, and its depletion suppresses tumorigenic phenotypes of breast cancer cell lines[10]. Knockdown of the mRNA and lncRNA methyltransferases METTL3 and METTL14 results in loss of stem cell self-renewal capability[13]. NSUN2, a tRNA RNMT that may also methylate lncRNAs, is induced by the oncogene c-Myc, stabilizes the mitotic spindle in fast cell proliferation, and depletion of NSUN2 selectively kills cancer cells[28-30]. Dozens of lncRNAs act as oncogenes such as ANRIL, HOTAIR or BCAR4 in

gastric, breast, and other cancer types[31-34], and targeting the methylation state of these molecules may reveal novel opportunities for therapy. To support nascent efforts towards the development of RNMT inhibitors, here, the structural chemistry landscape of human RNMTs is derived from available structures in the PDB. Structural mechanism of substrate recruitment, binding site geometry, druggability, and structural diversity are systematically analyzed, and opportunities and challenges for the chemical inhibition of RNMTs are discussed.

Box 1: RNMT glossary

- lncRNAs: long non-coding RNAs, longer than 200 nucleotides, involved in epigenetic signalling, splicing and other mechanisms that regulate gene expression and protein synthesis
- snRNAs: small nuclear RNAs, about 150 nucleotides in length, that participate in the splicing of mRNA and other RNA processing reactions
- snoRNAs: small nucleolar RNAs, a subgroup of snRNAs that guide site-specific rRNA modification
- miRNAs: microRNAs, about 22 nucleotides in length, involved in gene silencing
- piRNAs: Piwi-interacting RNAs, about 28 nucleotides long, involved in transposon silencing and epigenetic mechanisms
- RNA cap: modification, generally at the 5'end of RNA molecules in eukaryotes and viruses, that contribute to RNA stability and interaction with proteins
- Rossman-fold: common protein structure that generally binds nucleotides, acts as the catalytic domain of most human methyltransferases
- SPOUT: catalytic domain of a number of SAM-dependent methyltranferases found in eukaryotes and prokaryotes.
- SAM: S-adenosyl-methionine, methyl-donating cofactor of a large number of methyltransferases
- Druggability, ligandability: propensity of a protein cavity to act as a binding site for drug-like compounds, or small molecule ligands

Overall structure: Rossman fold or SPOUT domain

Of the 57 human RNMTs identified to date, five, six, 14 and 22 methylate mRNAs, small RNAs, rRNAs and tRNAs respectively, and 12 have unknown substrates. The structures of the catalytic domain of two mRNA-, three small RNA-, six rRNA-, four tRNA-methyltransterases, as well as one RNMT of unknown substrate were deposited in the PDB (Figure 2). These structures vary in size, conformation and quaternary arrangement, but can be divided into two general folds. The majority of RNMTs (43 out of 57) adopt a Rossman fold, typical of class I methyltransferases, and shared with protein arginine methyltransferases (PRMTs), some lysine methyltransferases such as DOT1L or CAMKMT, small molecule methyltransferases and DNMTs. Some of these enzymes may be able to methylate more than one type of substrate. For instance, FBL can methylate both rRNA and a glutamine side-chain of histone H2A.[35, 36] Four variable loop regions decorate the core Rossman fold and contribute to substrate recruitment (Figure 2). The length, sequence and secondary arrangement of these loops vary from one enzyme to another, producing substrate-binding sites that differ in size, shape and electrostatics, and establishing structural determinants for substrate specificity. For instance, loop L2, between β-strand 4 and helix D of the Rossman fold, is only 5-residue long in FBL (237-242), leaving the substrate binding site solvent exposed, but is 23 residue long in TGS1 (763-786) where it encloses the substrate (Figures 2 and 3). Flanking domains can also provide large basic surface areas, probably acting as RNA binding platforms, as observed in the rRNA m^6A methyltransferases DIMT1 and TFB1M or the rRNA m^5C methyltransferases NSUN5 (PDB codes 1ZQ9, 4GC9, 2B9E). Embellishment of the core Rossman fold with distinct loops and domains results in positioning of the 5'-terminal guanosine at the site of methyl transfer in the enzyme RNMT but at a different, juxtaposed cavity in CMTR1 (Figures 2 and 3). These additional domains can also be inserted within the Rossman fold, as is the case between β-strand 5 and helix E of the enzyme RNMT (PDB code 3BGV). Some Class-I RNMTs that lack these

additional RNA binding extensions need to be in complex with other proteins to be fully functional. For instance, the RNA binding protein MTERF4 interacts with and recruits NSUN4 to its rRNA substrate (PDB code 4FZV).[37]

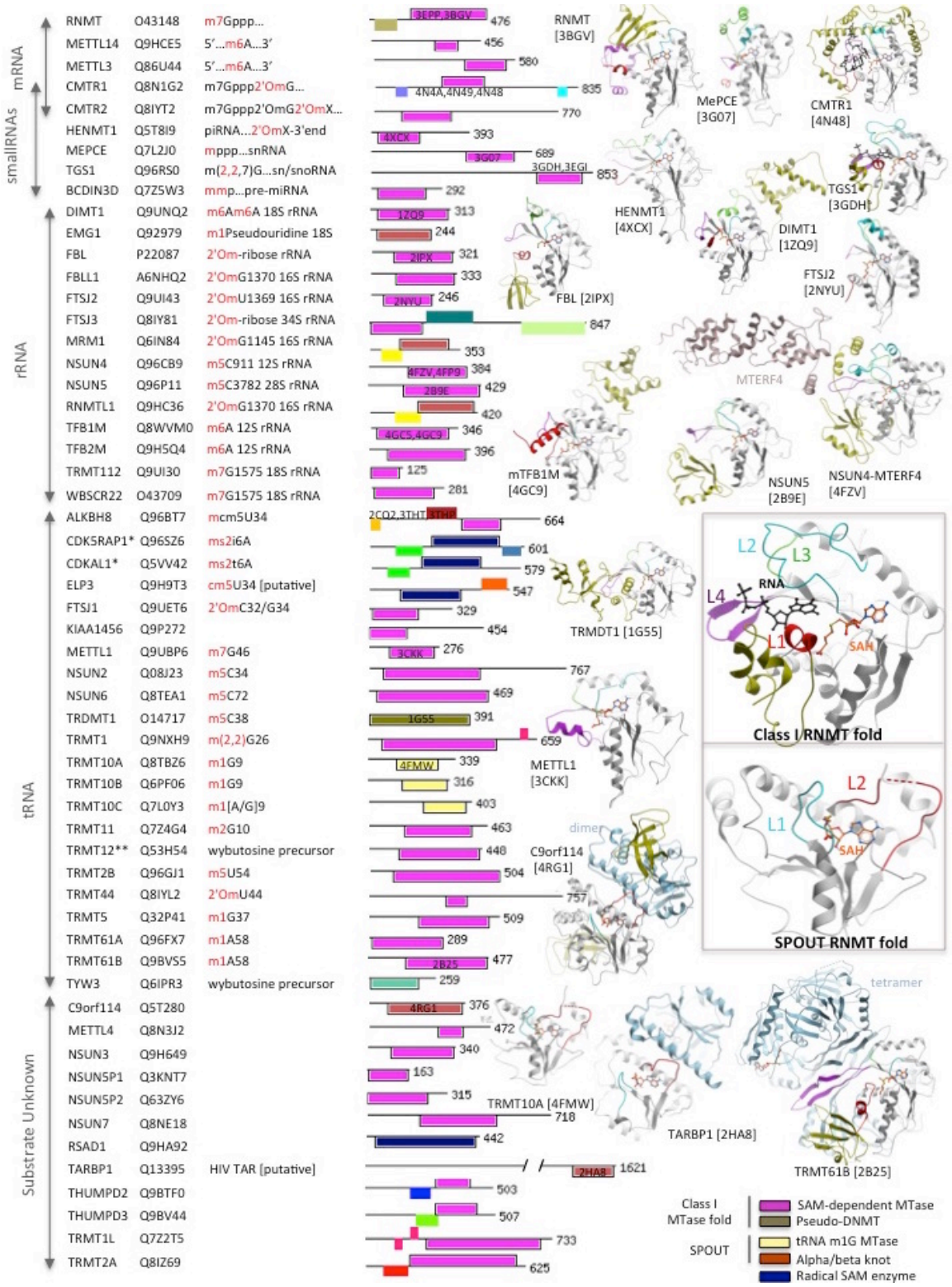

Figure 2: Substrate specificity and structure of human RNMTs. Name, Uniprot ID, substrate, domain architecture, and tertiary structures of human RNMTs are shown. When known, the methyl group transferred by the enzyme is indicated in red (ex: METTL14/METTL3 add a methyl group at

position 6 of adenine in the context of m7GpppA capped mRNAs). Structural coverage is indicated by PDB codes mapped onto domain architecture (catalytic methyltransferase domains are boxed – domain architecture is extracted from Uniprot). 3D structures include the catalytic core (gray), the cofactor (orange), variable loops contributing to the recruitment of the RNA substrate (Class I Mtase fold – loops L1-L4) or to SAM binding (SPOUT domain – loops L1, L2), other domains decorating the central core than may participate in binding RNA substrates (yellow), homo- or hetero-oligomeric subunits (sky blue, beige respectively), and bound RNA (black). 2'Om: methyl at the 2'-hyroxyl position of ribose. *:RNA methylthiotransferase; **: transfers an alpha-amino-alpha-carboxypropyl group from SAM. cm: carboxymethyl. X: any nucleotide. PDB codes indicate structures of human proteins except for TFB1M (mouse orthologue).

Non Rossman-fold RNMTs are organized around a SPOUT domain characterized by a knot structure at the cofactor-binding site.[38] Two canonical loops L1 and L2 vary in size and form a deep cofactor-binding pocket (Figure 2). While Rossman-fold RNMTs are generally monomeric, dimeric arrangements are observed in SPOUT methyltransferases, where the knot of one monomer is stabilized by the other monomer. Structural studies on non-human orthologs showed that the RNA substrate binds at the dimer interface.[39, 40]

The substrate-binding pocket is structurally diverse and opens widely on the cofactor site

S-adenosyl-methionine (SAM)-dependent methyltransferases transfer a methyl group from the cofactor SAM to a substrate. Cofactor and substrate binding sites of protein methyltransferases generally constitute two separate cavities that are linked by a short and narrow channel, making the development of dual competitors - compounds that occupy both sites – challenging. Unlike protein methyltransferases, most human RNMT structures available to date feature substrate and SAM binding sites that are merged into a large pocket, positively charged at the RNA-binding end. The development of chemical inhibitors that simultaneously exploit the cofactor and substrate binding cavities is therefore a promising strategy to target RNMTs, when both sites are shielded from solvent (Figure 3).

The enclosure of the substrate-binding cavity varies significantly among RNMTs. The binding sites of the methyl-accepting base of TGS1, TRDMT1, or the enzyme RNMT are enclosed (PDB codes 3GDH, 1G66, 3BGV). In each case, the substrate purine or pyrimidine is sandwiched between surrounding side-chains (or between RNMT and cofactor atoms in the case of TRDMT1), where a combination of hydrophobic interactions, pi-stacking and hydrogen bonds are observed (Figure 3, top). This base sandwiching mechanism is incompatible with the canonical base stacking of nucleic acid strands, suggesting an RNA binding mode for these enzymes where the substrate base would flip out of the RNA helix, as observed in the Nep1 RNMT structure bound to cognate RNA.[40] The methyl-accepting base is occupying a shallower, more solvent-exposed surface area in HENMT1, FBL and CMTR1 (PDB 4XCX, 2IPX, 4N48). In all cases, one face of the substrate base is stacked to neighboring nucleotides, preventing any insertion into enclosed binding sites (Figure 3, bottom). Intriguingly, the enzymes featuring an enclosed, more druggable substrate-binding cavity (TGS1, TRDMT1, and the enzyme RNMT) are all methylating purine or pyrimidine rings, while the shallow binding sites are all found in RNMTs methylating the ribose ring. As more structures become available, it will be interesting to see if this observation is fortuitous or has mechanistic implications.

While the methyl-accepting bases are occupying a shallow surface of HENMT1 and CMTR1, their 5'-flanking bases are inserted into enclosed cavities that may be chemically tractable (Figure 3, center). Targeting these sites juxtaposed to the catalytic center may be an avenue to antagonize catalytically competent positioning of the substrate.

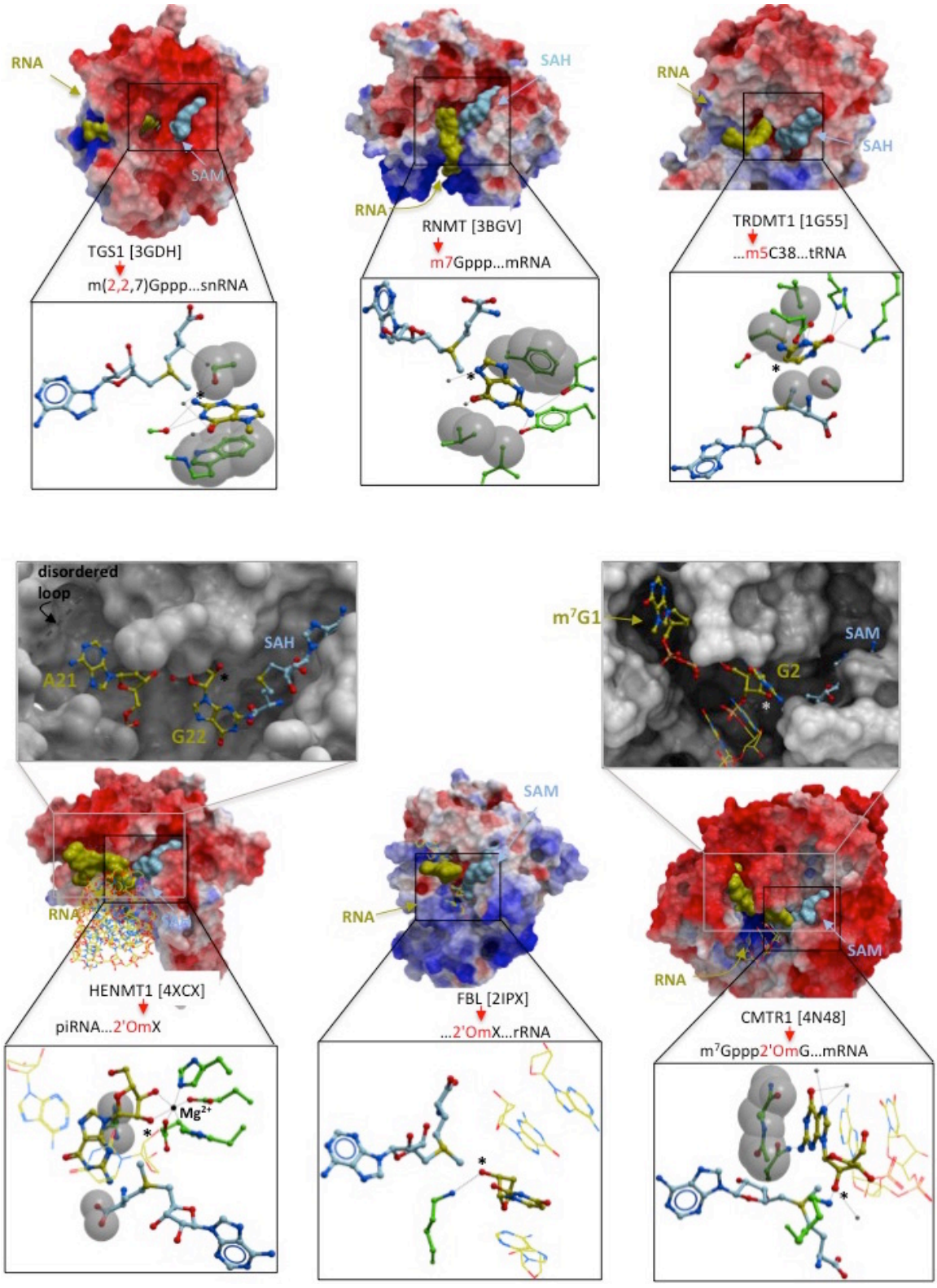

Figure 3. Substrate binding site of RNMTs. Coloring the Connolly surface of RNMTs according to their electrostatic potential (blue: positive, red: negative) shows that RNA substrates (yellow) bind

basic areas on the protein surface. Bases that are methylated at the purine or pyrimidine ring are sandwiched between aromatic or hydrophobic groups (black inserts, top), while ribonuclosides methylated at the ribose group are laying on shallow surfaces of the enzyme (black inserts, bottom). Ribonucleosides flanking the substrate are sometimes enclosed in more druggable cavities (grey inserts, middle). Connolly surfaces are all from structures of the human ortholog. Co-crystallized substrates were extracted from structures of orthologs when not available from human as follows. RNMT: substrate from fungus ortholog structure [1RI1] (3.5 Å rmsd with human [3BGV]). HENMT: substrate from plant ortholog structure [3HTX] (3.2Å rmsd with human [4XCX]). FBL: substrate from archae ortholog [3PLA] (1.5 Å rmsd with human [2IPX]). TRDMT1: substrate from bacterial homolog [2C7O] (residues within 6 Å of substrate cytosine: 3 Å rmsd with human [1G55]). A black asterisk indicates the methyl-accepting atom.

The cofactor-binding site is structurally diverse and not always druggable

Superimposing cofactor structures in their conformations bound to Rossman-fold RNA, DNA or protein methyltransferases reveals a highly conserved binding pose (Figure 4A, top). This bound conformation is strikingly different from the binding poses observed in SPOUT RNMTs or in SET-domain PMTs (Figure 4A, bottom). This ligand-based analysis suggests that cofactor competitive inhibitors should be selective between Class I methyltransferases, SPOUT RNMTs, and SET domain PMTs. Clustering human methyltransferases based on normalized structural distances between their cofactor binding sites defines the three same groups: Class I methyltransferases, SPOUT RNMTs, and SET domain PMTs (Figure 4B, top). This confirms a low risk of poly-pharmacology between these three groups of enzymes when targeting the cofactor site. To better appreciate the feasibility of selectively targeting a single enzyme, box plot representations of the ensemble of structural distances separating cofactor-binding sites were generated (Figure 4B, bottom). This reveals a greater structural diversity among Class I RNMTs (median distance [md] = 0.6) than among PRMTs (md = 0.1) or, to a lesser extent, among SET domain PMTs (md = 0.4). It was previously shown that the cofactor site of PMTs is structurally as diverse as the ATP site of kinases;[41] the present analysis suggests that the same is true for RNMTs. More details on any given RNMT structure can be found at thesgc.org/epigenetics_pocketome.[42]

To assess the ligandability of the cofactor-binding cavity, binding site enclosure and formal charges were calculated with ICM (Molsoft LLC). Less charged and more enclosed pockets are expected to be more druggable. At one end of the ligandability spectrum, the cofactor site of TRMT10A, a SPOUT RNMT, appears as particularly druggable: 11 hydrophobic side-chains and only two charged aminoacids are lining its mostly enclosed binding pocket (Figure 4C). The druggability of CMTR1 is not as clear, with a binding pocket partially enclosed and surrounded with 10 hydrophobic residues but also three aspartic acids and one lysine. The apo-CMTR1 structure reveals extensive conformational dynamics of loop regions at the cofactor site, a cautionary sign for structure-based ligand design (Figure 4D).[43] Significantly less druggable, the cofactor site of NSUN4 is mostly solvent exposed and lined with four aspartates, 2 arginines and one lysine. In these three examples, as in all other RNMTs, cofactor binding is relying on a dense network of direct and water-mediated hydrogen-bonds (Figure 4C). Surprisingly, in the DIMT1 structure, the amino-acid tail of SAM relocates at the substrate binding cavity, resulting in a less enclosed but more hydrophobic pocket (Figure 4C,E). A similar structural arrangement was previously described with PRMT5, a Rossman-fold PMT, and was exploited towards the development of a selective bi-substrate inhibitor.[44] This observation further supports the notion that bi-substrate inhibition could be a successful design strategy to inhibit RNMTs. The three SPOUT RNMTs included in this analysis, TRMT10A, C9orf114 and TARBP1 (PDB codes 4FMW, 4RG1, 2HA8 respectively), are predicted to have some of the most druggable cofactor binding pockets. This supports screening SPOUT RNMTs with chemical libraries focused on the cofactor site.

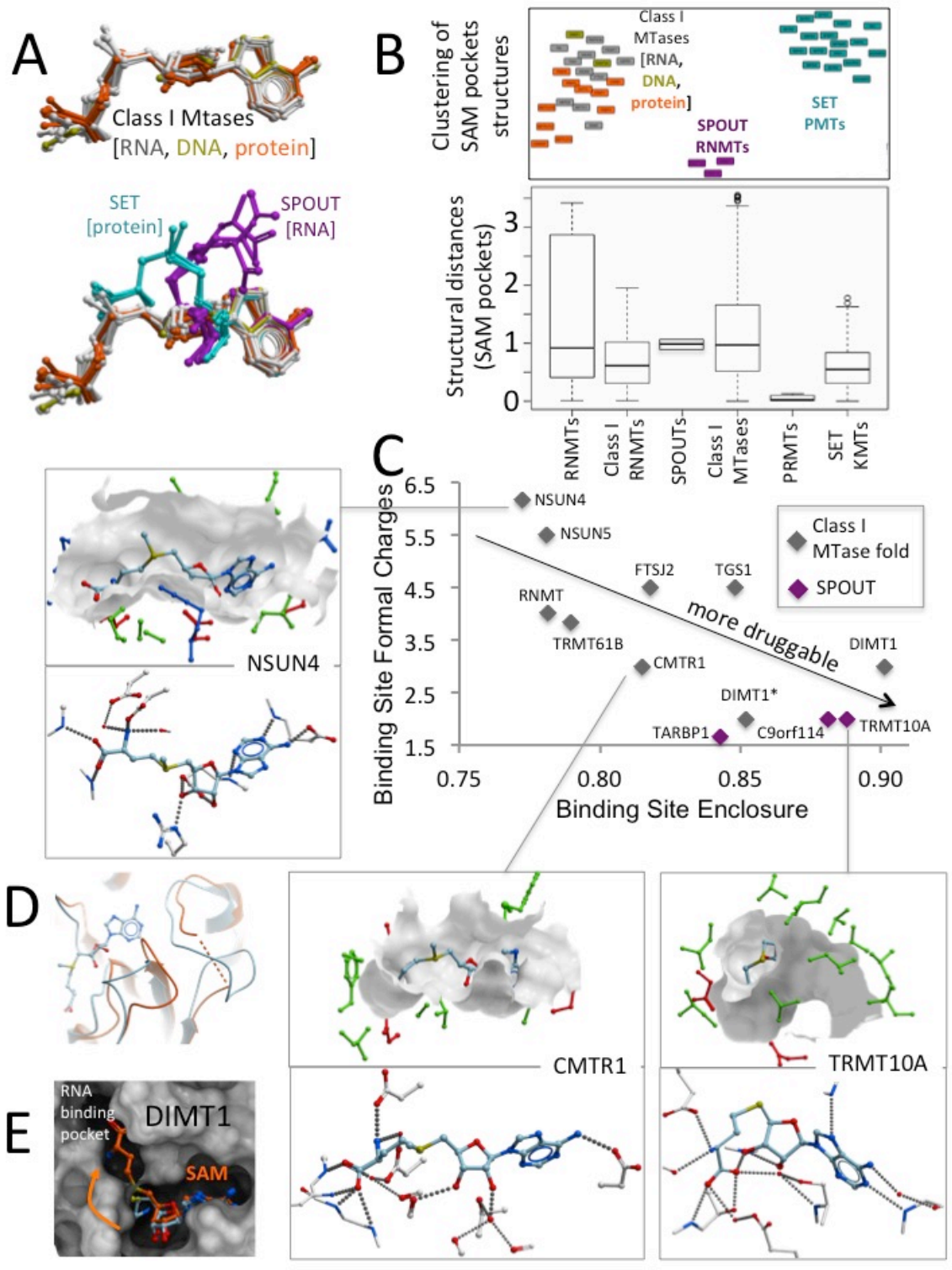

Figure 4: Cofactor binding site of RNMTs. Structural diversity: (**A)** the binding pose of SAM is conserved between RNA-, DNA-, and protein-methyltransferases sharing the Class I methyltransferase fold (top: superimposed structures of 11, 2, and 10 proteins are shown

respectively). SAM adopts a distinct conformation when bound to SPOUT RNMTs, which is also different from that observed in SET domain PMTs (bottom). **(B)** Clustering and boxplot distribution of RNA, DNA and protein methyltransferases based on the structural similarity of their cofactor binding pocket (structural distances calculated as in;[42] clustering produced by force-directed layout algorithm). **Druggability: (C)** The druggability of the cofactor site relies on its enclosure and hydrophobicity. (Side-chain color-coding: green: hydrophobic; red: positively charged; blue: negatively charged. Pocket enclosure is indicated with a white mesh). **Plasticity: (D)** Superimposed structures of apo (orange) and holo (sky blue) structures of CMTR1 (PDB 4N4A, 4N48). **(E)** The aminoacid end of the cofactor can relocate in the RNA binding site of DIMT1 (orange: SAM bound to human DIMT1 [1ZQ9]; sky blue: SAH bound to archaeal ortholog [3GRR]. Druggability parameters of the pocket exploited by the orange binding pose are highlighted with a star on the druggability plot). PDB codes of structures used: Class I RNMTs: CMTR1 [4N48], FTSJ2 [2NYU], MEPCE [3G07], METTL1 [3CKK], NSUN4 [4FP9], NSUN5 [2B9E], RNMT [3BGV], TGS1 [3GDH], TRDMT1 [1G55], TRMT61B [2B25]. SPOUT: C9orf114 [4RG1], TARBP1 [2HA8], TRMT10A [4FMW]. SET domain PMTs: ASH1L [3OPE], EHMT1 [2IGQ], EHMT2 [2O8J], MLL [2W5Y], NSD1 [3OOI], SETD2 [4FMU], SETD3 [3SMT], SETD6 [3QXY], SETD7 [1MT6], SETD8 [1ZKK], SETMAR [3BO5], SMYD1 [3N71], SMYD2 [3TG4], SMYD3 [3MEK], SUV39H2 [2R3A], SUV420H1 [3S8P], SUV420H2 [3RQ4]. Class I PMTs: CAMKMT [4PWY], CARM1 [2V74], DOT1L [1NW3], METTL21A [4LEC], METTL21C [4MTL], METTL21D [4LG1], PRMT1 [1OR8], PRMT3 [2FYT], PRMT5 [4GQB], PRMT6 [4HC4]. DNMTs: DNMT1 [3PTA], DNMT3A [2QRV]. The hDIMT1 structure was not included in B as residues lining SAM do not reflect the real cofactor binding site. TRDMT1, METTL1 and MEPCE were not included in (C) as the cofactor site is not complete in these structures.

CONCLUSION

Human RNMTs constitute a promising protein family for drug discovery. The development of an RNMT-focused chemistry toolbox, and the discovery of potent, selective, cell-active chemical probes to interrogate the cellular function of these enzymes are necessary steps towards the establishment of RNMTs as a valid target class for therapy. The purpose of the structural chemistry landscape drawn here is to provide the medicinal chemistry community with a preliminary structural analysis that may inform the discovery of the first human RNMT inhibitors.

ACKNOWLEDGMENTS

Thank you to Dr. Hazem Ahmed for the figure on the clustering of SAM pocket structures. The SGC is a registered charity (number 1097737) that receives funds from AbbVie, Bayer Pharma AG, Boehringer Ingelheim, Canada Foundation for Innovation, Eshelman Institute for Innovation, Genome Canada, Innovative Medicines Initiative (EU/EFPIA) [ULTRA-DD grant no. 115766], Janssen, Merck & Co., Novartis Pharma AG, Ontario Ministry of Economic Development and Innovation, Pfizer, São Paulo Research Foundation-FAPESP, Takeda, and the Wellcome Trust.

REFERENCES:

1. Byszewska, M., Smietanski, M., Purta, E., and Bujnicki, J. M. (2014) RNA methyltransferases involved in 5' cap biosynthesis, *RNA Biol 11*, 1597-1607.
2. Dunin-Horkawicz, S., Czerwoniec, A., Gajda, M. J., Feder, M., Grosjean, H., and Bujnicki, J. M. (2006) MODOMICS: a database of RNA modification pathways, *Nucleic Acids Res 34*, D145-149.
3. Wang, X., and He, C. (2014) Dynamic RNA modifications in posttranscriptional regulation, *Mol Cell 56*, 5-12.
4. Ghosh, A., and Lima, C. D. (2010) Enzymology of RNA cap synthesis, *Wiley Interdiscip Rev RNA 1*, 152-172.
5. Gonatopoulos-Pournatzis, T., Dunn, S., Bounds, R., and Cowling, V. H. (2011) RAM/Fam103a1 is required for mRNA cap methylation, *Mol Cell 44*, 585-596.
6. Werner, M., Purta, E., Kaminska, K. H., Cymerman, I. A., Campbell, D. A., Mittra, B., Zamudio, J. R., Sturm, N. R., Jaworski, J., and Bujnicki, J. M. (2011) 2'-O-ribose methylation of cap2 in human: function and evolution in a horizontally mobile family, *Nucleic Acids Res 39*, 4756-4768.
7. Belanger, F., Stepinski, J., Darzynkiewicz, E., and Pelletier, J. (2010) Characterization of hMTr1, a human Cap1 2'-O-ribose methyltransferase, *J Biol Chem 285*, 33037-33044.
8. Monecke, T., Dickmanns, A., and Ficner, R. (2009) Structural basis for m7G-cap hypermethylation of small nuclear, small nucleolar and telomerase RNA by the dimethyltransferase TGS1, *Nucleic Acids Res 37*, 3865-3877.
9. Jeronimo, C., Forget, D., Bouchard, A., Li, Q., Chua, G., Poitras, C., Therien, C., Bergeron, D., Bourassa, S., Greenblatt, J., Chabot, B., Poirier, G. G., Hughes, T. R., Blanchette, M., Price, D. H., and Coulombe, B. (2007) Systematic analysis of the protein interaction network for the human transcription machinery reveals the identity of the 7SK capping enzyme, *Mol Cell 27*, 262-274.
10. Xhemalce, B., Robson, S. C., and Kouzarides, T. (2012) Human RNA methyltransferase BCDIN3D regulates microRNA processing, *Cell 151*, 278-288.

11. Kirino, Y., and Mourelatos, Z. (2007) The mouse homolog of HEN1 is a potential methylase for Piwi-interacting RNAs, *RNA 13*, 1397-1401.
12. Liu, N., and Pan, T. (2015) RNA epigenetics, *Transl Res 165*, 28-35.
13. Wang, Y., Li, Y., Toth, J. I., Petroski, M. D., Zhang, Z., and Zhao, J. C. (2014) N6-methyladenosine modification destabilizes developmental regulators in embryonic stem cells, *Nat Cell Biol 16*, 191-198.
14. Jia, G., Fu, Y., Zhao, X., Dai, Q., Zheng, G., Yang, Y., Yi, C., Lindahl, T., Pan, T., Yang, Y. G., and He, C. (2011) N6-methyladenosine in nuclear RNA is a major substrate of the obesity-associated FTO, *Nat Chem Biol 7*, 885-887.
15. Wang, X., Lu, Z., Gomez, A., Hon, G. C., Yue, Y., Han, D., Fu, Y., Parisien, M., Dai, Q., Jia, G., Ren, B., Pan, T., and He, C. (2014) N6-methyladenosine-dependent regulation of messenger RNA stability, *Nature 505*, 117-120.
16. Wang, X., Zhao, B. S., Roundtree, I. A., Lu, Z., Han, D., Ma, H., Weng, X., Chen, K., Shi, H., and He, C. (2015) N(6)-methyladenosine Modulates Messenger RNA Translation Efficiency, *Cell 161*, 1388-1399.
17. Zheng, G., Dahl, J. A., Niu, Y., Fedorcsak, P., Huang, C. M., Li, C. J., Vagbo, C. B., Shi, Y., Wang, W. L., Song, S. H., Lu, Z., Bosmans, R. P., Dai, Q., Hao, Y. J., Yang, X., Zhao, W. M., Tong, W. M., Wang, X. J., Bogdan, F., Furu, K., Fu, Y., Jia, G., Zhao, X., Liu, J., Krokan, H. E., Klungland, A., Yang, Y. G., and He, C. (2013) ALKBH5 is a mammalian RNA demethylase that impacts RNA metabolism and mouse fertility, *Mol Cell 49*, 18-29.
18. Liu, N., Dai, Q., Zheng, G., He, C., Parisien, M., and Pan, T. (2015) N(6)-methyladenosine-dependent RNA structural switches regulate RNA-protein interactions, *Nature 518*, 560-564.
19. Squires, J. E., Patel, H. R., Nousch, M., Sibbritt, T., Humphreys, D. T., Parker, B. J., Suter, C. M., and Preiss, T. (2012) Widespread occurrence of 5-methylcytosine in human coding and non-coding RNA, *Nucleic Acids Res 40*, 5023-5033.
20. Piekna-Przybylska, D., Decatur, W. A., and Fournier, M. J. (2008) The 3D rRNA modification maps database: with interactive tools for ribosome analysis, *Nucleic Acids Res 36*, D178-183.
21. Song, X., and Nazar, R. N. (2002) Modification of rRNA as a 'quality control mechanism' in ribosome biogenesis, *FEBS Lett 523*, 182-186.
22. Decatur, W. A., and Fournier, M. J. (2002) rRNA modifications and ribosome function, *Trends Biochem Sci 27*, 344-351.
23. Agris, P. F. (2004) Decoding the genome: a modified view, *Nucleic Acids Res 32*, 223-238.
24. El Yacoubi, B., Bailly, M., and de Crecy-Lagard, V. (2012) Biosynthesis and function of posttranscriptional modifications of transfer RNAs, *Annu Rev Genet 46*, 69-95.
25. Hopper, A. K. (2013) Transfer RNA post-transcriptional processing, turnover, and subcellular dynamics in the yeast Saccharomyces cerevisiae, *Genetics 194*, 43-67.
26. Lim, S. P., Sonntag, L. S., Noble, C., Nilar, S. H., Ng, R. H., Zou, G., Monaghan, P., Chung, K. Y., Dong, H., Liu, B., Bodenreider, C., Lee, G., Ding, M., Chan, W. L., Wang, G., Jian, Y. L., Chao, A. T., Lescar, J., Yin, Z., Vedananda, T. R., Keller, T. H., and Shi, P. Y. (2011) Small molecule inhibitors that selectively block dengue virus methyltransferase, *J Biol Chem 286*, 6233-6240.
27. Podvinec, M., Lim, S. P., Schmidt, T., Scarsi, M., Wen, D., Sonntag, L. S., Sanschagrin, P., Shenkin, P. S., and Schwede, T. (2010) Novel inhibitors of dengue virus

methyltransferase: discovery by in vitro-driven virtual screening on a desktop computer grid, *J Med Chem 53*, 1483-1495.
28. Hussain, S., Sajini, A. A., Blanco, S., Dietmann, S., Lombard, P., Sugimoto, Y., Paramor, M., Gleeson, J. G., Odom, D. T., Ule, J., and Frye, M. (2013) NSun2-mediated cytosine-5 methylation of vault noncoding RNA determines its processing into regulatory small RNAs, *Cell Rep 4*, 255-261.
29. Hussain, S., Benavente, S. B., Nascimento, E., Dragoni, I., Kurowski, A., Gillich, A., Humphreys, P., and Frye, M. (2009) The nucleolar RNA methyltransferase Misu (NSun2) is required for mitotic spindle stability, *J Cell Biol 186*, 27-40.
30. Frye, M., and Watt, F. M. (2006) The RNA methyltransferase Misu (NSun2) mediates Myc-induced proliferation and is upregulated in tumors, *Curr Biol 16*, 971-981.
31. Gupta, R. A., Shah, N., Wang, K. C., Kim, J., Horlings, H. M., Wong, D. J., Tsai, M. C., Hung, T., Argani, P., Rinn, J. L., Wang, Y., Brzoska, P., Kong, B., Li, R., West, R. B., van de Vijver, M. J., Sukumar, S., and Chang, H. Y. (2010) Long non-coding RNA HOTAIR reprograms chromatin state to promote cancer metastasis, *Nature 464*, 1071-1076.
32. Xing, Z., Lin, A., Li, C., Liang, K., Wang, S., Liu, Y., Park, P. K., Qin, L., Wei, Y., Hawke, D. H., Hung, M. C., Lin, C., and Yang, L. (2014) lncRNA directs cooperative epigenetic regulation downstream of chemokine signals, *Cell 159*, 1110-1125.
33. Zhang, E. B., Kong, R., Yin, D. D., You, L. H., Sun, M., Han, L., Xu, T. P., Xia, R., Yang, J. S., De, W., and Chen, J. (2014) Long noncoding RNA ANRIL indicates a poor prognosis of gastric cancer and promotes tumor growth by epigenetically silencing of miR-99a/miR-449a, *Oncotarget 5*, 2276-2292.
34. Sahu, A., Singhal, U., and Chinnaiyan, A. (2015) Long noncoding RNAs in cancer: from function to translation, *Trends in Cancer 1*, 93-109.
35. Tessarz, P., Santos-Rosa, H., Robson, S. C., Sylvestersen, K. B., Nelson, C. J., Nielsen, M. L., and Kouzarides, T. (2014) Glutamine methylation in histone H2A is an RNA-polymerase-I-dedicated modification, *Nature 505*, 564-568.
36. Tollervey, D., Lehtonen, H., Jansen, R., Kern, H., and Hurt, E. C. (1993) Temperature-sensitive mutations demonstrate roles for yeast fibrillarin in pre-rRNA processing, pre-rRNA methylation, and ribosome assembly, *Cell 72*, 443-457.
37. Yakubovskaya, E., Guja, K. E., Mejia, E., Castano, S., Hambardjieva, E., Choi, W. S., and Garcia-Diaz, M. (2012) Structure of the essential MTERF4:NSUN4 protein complex reveals how an MTERF protein collaborates to facilitate rRNA modification, *Structure 20*, 1940-1947.
38. Tkaczuk, K. L., Dunin-Horkawicz, S., Purta, E., and Bujnicki, J. M. (2007) Structural and evolutionary bioinformatics of the SPOUT superfamily of methyltransferases, *BMC Bioinformatics 8*, 73.
39. Ito, T., Masuda, I., Yoshida, K., Goto-Ito, S., Sekine, S., Suh, S. W., Hou, Y. M., and Yokoyama, S. (2015) Structural basis for methyl-donor-dependent and sequence-specific binding to tRNA substrates by knotted methyltransferase TrmD, *Proc Natl Acad Sci U S A 112*, E4197-4205.
40. Thomas, S. R., Keller, C. A., Szyk, A., Cannon, J. R., and Laronde-Leblanc, N. A. (2011) Structural insight into the functional mechanism of Nep1/Emg1 N1-specific pseudouridine methyltransferase in ribosome biogenesis, *Nucleic Acids Res 39*, 2445-2457.

41. Campagna-Slater, V., Mok, M. W., Nguyen, K. T., Feher, M., Najmanovich, R., and Schapira, M. (2011) Structural chemistry of the histone methyltransferases cofactor binding site, *J Chem Inf Model 51*, 612-623.
42. Cabaye, A., Nguyen, K. T., Liu, L., Pande, V., and Schapira, M. (2015) Structural diversity of the epigenetics pocketome, *Proteins*.
43. Smietanski, M., Werner, M., Purta, E., Kaminska, K. H., Stepinski, J., Darzynkiewicz, E., Nowotny, M., and Bujnicki, J. M. (2014) Structural analysis of human 2'-O-ribose methyltransferases involved in mRNA cap structure formation, *Nat Commun 5*, 3004.
44. Smil, D., Eram, M. S., Li, F., Kennedy, S., Szewczyk, M. M., Brown, P. J., Barsyte-Lovejoy, D., Arrowsmith, C. H., Vedadi, M., and Schapira, M. (2015) Discovery of a Dual PRMT5-PRMT7 Inhibitor, *ACS Med Chem Lett 6*, 408-412.

TOC Graphic

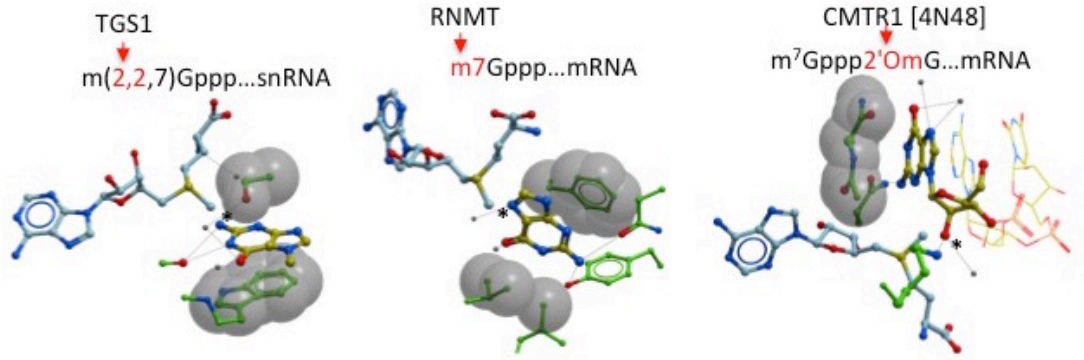
TGS1
m(2,2,7)Gppp…snRNA
RNMT
m7Gppp…mRNA
CMTR1 [4N48]
m7Gppp2'OmG…mRNA